Proceedings of the International Workshop NOA'00, Grybów 2000

COLLISION-TIME ASYMMETRY AND SPEED-DEPENDENT EFFECTS ON THE ^{114}Cd 326.1 nm LINE PERTURBED BY Kr

R.S. Trawiński, A. Bielski and D. Lisak

Institute of Physics, Nicholas Copernicus University
Grudziądzka 5/7, 87-100 Toruń, Poland

(Received December 7, 2000; revised version January 30, 2001)

Using a laser-induced fluorescence method, detailed analysis of profiles of the ^{114}Cd 326.1 nm line perturbed by krypton was performed which revealed departures from the ordinary Voigt profile. These departures are shown to be consistent with fits of experimental profiles to a speed-dependent asymmetric Voigt profile. Coefficients of the pressure broadening, shift, and collision-time asymmetry are determined and compared with those calculated in the adiabatic approximation for the van der Waals, Czuchaj–Stoll, and Morse potentials.

PACS numbers: 32.70.–n, 33.70.–w, 34.20.–b

1. Introduction

In an earlier paper [1] from this laboratory, hereafter referred to as I, we reported observations showing that the shape in the core region of the 326.1 nm ^{114}Cd intercombination line perturbed by Kr contains dispersion component in addition to the ordinary Lorentzian. The physical origin of this component was found to be finite duration of the collisions in accordance with theoretical predictions of Anderson and Talman [2], Szudy and Baylis [3], Al-Saqabi and Peach [4], and others (see e.g. [5, 6]). The appearance of the dispersion-shaped component causes the resulting line profile to become asymmetric and this type of asymmetry hereafter will be referred to as collision-time asymmetry. It is often accompanied by other asymmetry features arising from the correlation between the collision and Doppler broadening [7, 8] due to the dependence of collisional characteristics on the speed of the emitting (or absorbing) atom. Berman [7] and Ward et al. [8] have shown that the collision-Doppler correlation can be neglected only in the case when the emitter mass m_{E} is much greater than the mass of the perturber m_{P}, i.e. for systems corresponding to very small values of $\alpha = m_{\mathrm{P}}/m_{\mathrm{E}}$, the ratio of perturber and emitter masses. For such systems and in the impact limit when the collision duration is assumed to be negligibly small the resulting line shape can be described by the well-known Voigt profile (VP) which is a convolution of Lorentzian and Gaussian profiles. If, however, for systems with small α-values the finite duration of collision is taken into account, then in the first approximation the line shape can be described by the asymmetric Voigt profile (AVP), i.e. a convolution of the Gaussian profile with a profile represented by the sum of the Lorentzian and dispersion profiles [6, 7, 9].

For systems consisting of heavy perturbers and light emitters ($\alpha > 1$) collision correlation effects become increasingly apparent with increasing value of α. To include these effects in the impact limit the Lorentzian profile with speed-dependent width (FWHM) $\gamma_L(v_E)$ and shift $\Delta(v_E)$ must be averaged correctly over emitter velocities (v_E) using the Maxwellian distribution. Following Berman [7] such velocity-averaged impact profile will be referred to as the speed-dependent Voigt profile (SDVP). Beyond the impact limit the dispersion-shaped correction to the Lorentzian component should be taken into account which must similarly be averaged over velocities and following Harris et al. [9] profiles obtained in such a way will be referred to as the speed-dependent asymmetric Voigt profile (SDAVP).

In another paper [10], hereafter referred to as II, we used a laser-induced fluorescence (LIF) technique to study the influence of speed-dependent effects caused by Xe on the profile of the Cd 326.1 nm intercombination line. The good signal-to-noise ratio and negligible instrumental profile enabled us to identify deviations of our measured line profile from the ordinary Voigt profile (VP). We have found that for Cd–Xe besides the effect of the finite collision duration also speed-dependent effects leading to the correlation between pressure broadening rate and thermal motion of emitting atoms must be taken into account. Moreover, the SDAVP expression derived by Harris et al. [9, 11] which includes these corrections describes the experimental profile to a much greater degree of accuracy than ordinary VP expression.

The goal of the present work was to verify whether the speed-dependent effects can also be experimentally found for systems with smaller value of α, the ratio of perturber and emitter masses, such as e.g. Cd–Kr ($\alpha = 0.73$). We should note that in our preliminary experiments [12] dealing with the perturbation of the 326.1 nm Cd by Kr performed by means of classical emission spectroscopy using a pressure-scanned Fabry–Perot interferometer (FPI) neither collision-time asymmetry nor the Doppler-collision correlation effects have been found. Due to small transmission of the FPI, being its inherent feature, and the weakness of the fluorescence signal the line shape measurements described in Ref. [12] were possible only for Kr pressure below 100 Torr at room temperature. As was verified by our experimental tests and numerical simulations under these conditions for Cd–Kr it was practically impossible to observe any deviations from the ordinary VP since both the collision-time asymmetry and Doppler-collision correlation effects as very small effects are totally obscured by a periodic instrumental function of the FPI.

Contrary to that, in I the dispersion-shaped correction to the Lorentzian profile of the 326.1 nm Cd line perturbed by Kr was observed using a classical absorption method and interpreted as resulting from the finite collision duration. On the other side, however, no speed-dependent effects have been found for Cd–Kr in I. It should be noted that absorption measurements reported in I could be affected by a systematic error due to incomplete knowledge of the instrumental function of the scanning monochromator. Because of the similarity between contributions from collision duration and speed-dependent correlation effects an extreme care is required in any experimental study dealing with quantitative estimation of contributions from these two sources. For this reason we thought it necessary to carry out new measurements of the profiles of the ^{114}Cd 326.1 nm line perturbed by Kr using a laser-induced fluorescence technique.

The present research was also stimulated by recent theoretical work of Czuchaj and Stoll [13] who performed *ab initio* calculations of potential energy curves for Cd–rare gas systems, as well as by recent experimental studies of Cd–Kr excimers created in free supersonic expansion [14] in which spectroscopic constants for CdKr molecule were determined assuming the Morse potential.

2. Experimental setup

In order to avoid the hyperfine and isotopic structure of the Cd 326.1 nm line we used the ^{114}Cd isotope. The side-arm quartz cells containing ^{114}Cd isotope were filled with krypton and cut off from the vacuum system. The krypton pressure was varied between 5 and 430 Torr at room temperature. The cells were situated in the multisection oven enabling the independent temperature stabilization of the cell and its side arm up to 1 K. During the measurement the temperature of the cell was 724 K, while the temperature of its side arm was 440 K.

The line shape of the ^{114}Cd 326.1 nm line was registered using the LIF technique by means of a digital laser spectrometer described in earlier paper [15]. An actively stabilized single-frequency Coherent CR 899-21 ring dye laser equipped with intracavity frequency doubler, operating on DCM dye was pumped by INNOVA-400 argon-ion laser. The ring laser provided single mode UV output continuously tunable for up to 60 GHz with line width about 1 MHz. The intensity of fluorescence signal was measured by a thermoelectrically cooled photomultiplier working in the photon counting mode. Frequency calibration of the ring laser was performed using its fundamental (red) line directed to a confocal FPI with a free spectral range of 1.5 GHz and the 100 cm long iodine cell operated at temperature 35°C. The FPI transmission peaks and I_2 absorption spectrum were recorded simultaneously with the fluorescence signal for frequency calibration. The laser UV beam incident on the cell was linearly polarized in the vertical direction and the collection optics arm, perpendicular to the laser beam direction, contained a linear polarizer set at the "magic angle" (rotated 54.7° from the vertical), so the collection optics system was insensitive to effects due to anisotropy of fluorescence (see e.g. [16, 17]). All the data: fluorescence signal, laser UV output power, FPI transmission peaks and I_2 absorption spectrum were acquired with a PC computer for further evaluation.

3. Data analysis and results

Profiles of the ^{114}Cd 326.1 nm line were registered at a range of Kr density up to 1.4×10^{19} cm^{-3}. The experimental intensity distributions were fitted directly to all theoretical profiles discussed in paper II, i.e. ordinary VP, SDVP, AVP, and SDAVP.

The SDAVP profile may be written in the form

$$I_{\mathrm{SDAVP}}(\widetilde{\nu}) = \frac{1}{\pi}\int \mathrm{d}^3\boldsymbol{v}_{\mathrm{E}} f_{m_{\mathrm{E}}}(\boldsymbol{v}_{\mathrm{E}})$$

$$\times\frac{\frac{\gamma_{\mathrm{L}}}{2}B_{\mathrm{W}}(x;\alpha)+\chi B_{\mathrm{A}}(x;\alpha)\left[\widetilde{\nu}-\widetilde{\nu}_0-\varDelta B_{\mathrm{S}}(x;\alpha)-\frac{\boldsymbol{k}\boldsymbol{v}_{\mathrm{E}}}{2\pi c}\right]}{\left[\frac{\gamma_{\mathrm{L}}}{2}B_{\mathrm{W}}(x;\alpha)\right]^2+\left[\widetilde{\nu}-\widetilde{\nu}_0-\varDelta B_{\mathrm{S}}(x;\alpha)-\frac{\boldsymbol{k}\boldsymbol{v}_{\mathrm{E}}}{2\pi c}\right]^2}, \qquad (1)$$

where γ_{L}, $\varDelta$, and χ are the collisional line width, line shift, and collision-time asymmetry parameter, respectively, averaged over the Maxwellian distribution of the emitter velocities $f_{m_{\mathrm{E}}}(\boldsymbol{v}_{\mathrm{E}})$. The value $\boldsymbol{k}\boldsymbol{v}_{\mathrm{E}}/2\pi c$, where $\boldsymbol{k}$ is the wave vector of the emitted radiation and c is the speed of light, describes the Doppler shift of the unperturbed wave number $\widetilde{\nu}_0$. The half width of the Doppler (Gaussian) component of the line shape equals to $\gamma_{\mathrm{D}} = 2\sqrt{\ln 2}kv_{m_{\mathrm{E}}}$ where $v_{m_{\mathrm{E}}} = \sqrt{2k_{\mathrm{B}}T/m_{\mathrm{E}}}$ is the most probable emitter speed, T is the gas temperature and k_B is Boltzmann's constant. In Eq. (1) $x = v_{\mathrm{E}}/v_{m_{\mathrm{E}}}$ is the reduced emitter velocity.

The reduced Lorentzian width $B_{\mathrm{W}}(x;\alpha) = \gamma_{\mathrm{L}}(xv_{m_{\mathrm{E}}})/\gamma_{\mathrm{L}}$ and reduced pressure shift $B_{\mathrm{S}}(x;\alpha) = \varDelta(xv_{m_{\mathrm{E}}})/\varDelta$ functions were calculated using a method developed by Ward et al. [8], whereas the reduced collision-time asymmetry parameter $B_{\mathrm{A}}(x;\alpha) = \chi(xv_{m_{\mathrm{E}}})/\chi$ was calculated from an expression derived by Ciuryło et al. [18, 19]. These calculations were performed assuming van der Waals and Czuchaj–Stoll [13] potentials.

In appropriate limiting cases the SDAVP profile, Eq. (1), yields well-known profiles used in traditional line shape analysis. The neglect of speed-dependent effects which is justified for small α values, leads to AVP simply by putting $B_{\mathrm{W}}(x;\alpha) = B_{\mathrm{S}}(x;\alpha) = B_{\mathrm{A}}(x;\alpha) = 1$ in Eq. (1). On the other hand, the neglect of the collision-time asymmetry, leads to SDVP [7] simply by putting $\chi = 0$ in Eq. (1). The neglect of the both above effects leads to the ordinary VP.

Numerical fit of experimental profiles to VP as well as to SDVP allowed three parameters to vary: the Lorentzian width γ_{L}, the pressure shift $\varDelta$, and the Gaussian width γ_{D}. For AVP and SDAVP we also fitted the collision-time asymmetry parameter χ.

Figure 1a shows an example of the shape of the 326.1 nm ^{114}Cd line perturbed by Kr at 430 Torr at room temperature. The best fit profile SDAVP is plotted as the solid line. In order to examine the quality of the fits we used the weighted differences of the intensities

$$D_\sigma(\widetilde{\nu}) = \frac{I_{\mathrm{exp}}(\widetilde{\nu}) - I_{\mathrm{fit}}(\widetilde{\nu})}{\sqrt{I_{\mathrm{fit}}(\widetilde{\nu})}}, \qquad (2)$$

between measured $I_{\mathrm{exp}}(\widetilde{\nu})$ and fitted (theoretical) $I_{\mathrm{fit}}(\widetilde{\nu})$ profiles. As in our measurements, the intensity distribution was monitored using a photomultiplier working in the photon counting mode so the standard deviation corresponding to the

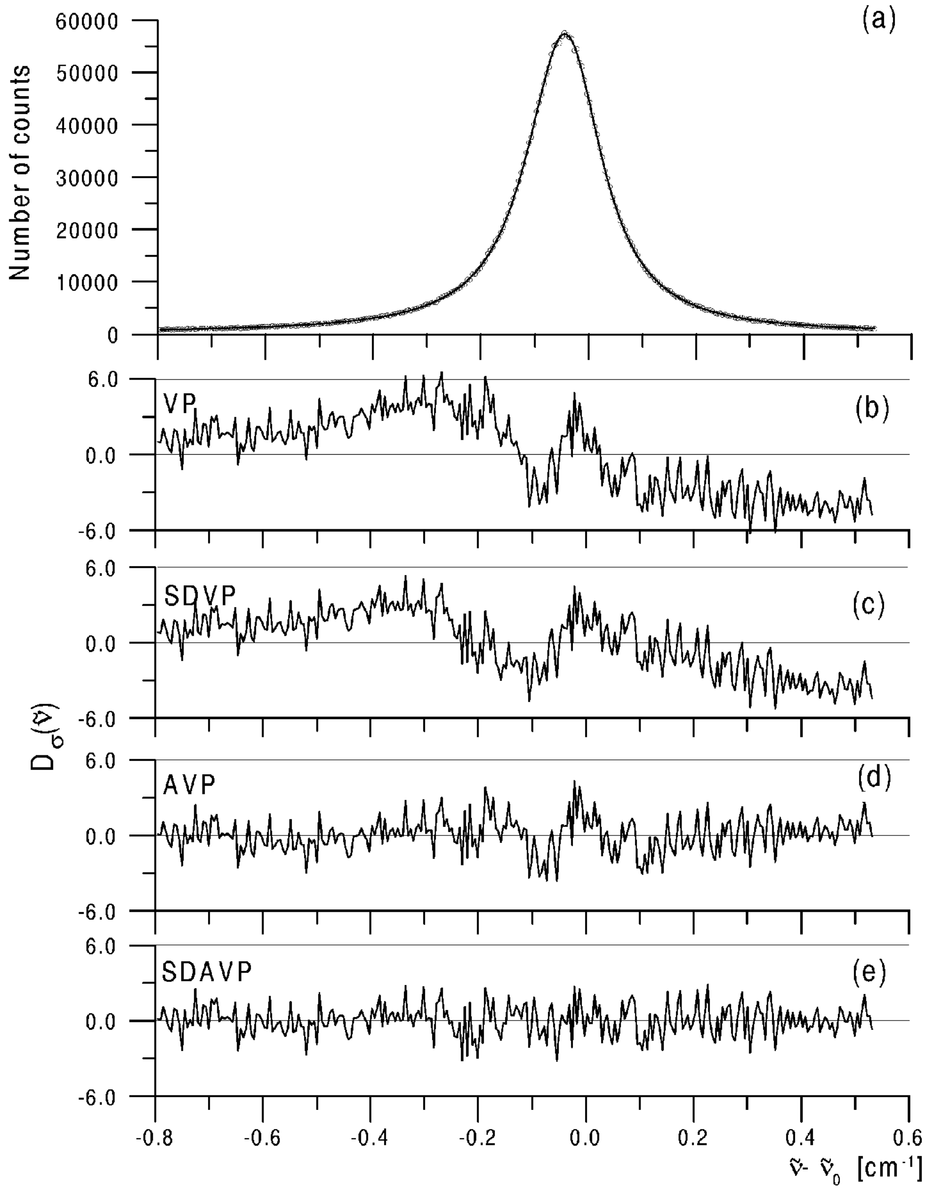

Fig. 1. The shape of the Cd 326.1 nm line perturbed by Kr at pressure 430 Torr: (a) experimental points together with the best-fit SDAVP (with Czuchaj and Stoll potential) (full curve), (b)–(e) weighted differences $D_\sigma(\widetilde{\nu})$ between experimental and fitted VP, SDVP, AVP, and SDAVP profiles, respectively.

best fit value at wave number $\tilde{\nu}$ is equal to $\sqrt{I_{\text{fit}}(\tilde{\nu})}$. In Fig. 1b we plotted these differences for the case when $I_{\text{fit}}(\tilde{\nu}) = \text{VP}$. We started the analysis with the ordinary Voigt profile since in this case the fit procedure reveals all the departures. We can see systematic departures from zero in the line core as well as on line wings which can be regarded as a manifestation of the line asymmetry. Figure 1c shows the differences for the case when $I_{\text{fit}}(\tilde{\nu}) = \text{SDVP}$. The systematic departures are still present on the line wings, while in the line core the quality of the fit is a little better. The departure due to the line asymmetry is lower because the SDVP includes the asymmetry arising from the correlation between the collision and Doppler broadening [7].

For $I_{\text{fit}}(\tilde{\nu}) = \text{AVP}$ (Fig. 1d) an improvement of the fit was obtained mainly on line wings. Figure 1e shows the differences for the case when $I_{\text{fit}}(\tilde{\nu}) = \text{SDAVP}$. As can be seen in this case, the values of the differences are spread uniformly about zero which confirms the goodness of the fit. It is thus seen that in the case of the Cd–Kr system both the collision-time asymmetry and speed-dependent effects have a noticeable influence on the profile of the 326.1 nm line.

In the following we are going to focus our attention on the problem how to distinguish these two effects which both can lead to asymmetry of the profile. Therefore in our analysis described in following sections we use the AVP and SDAVP profiles only.

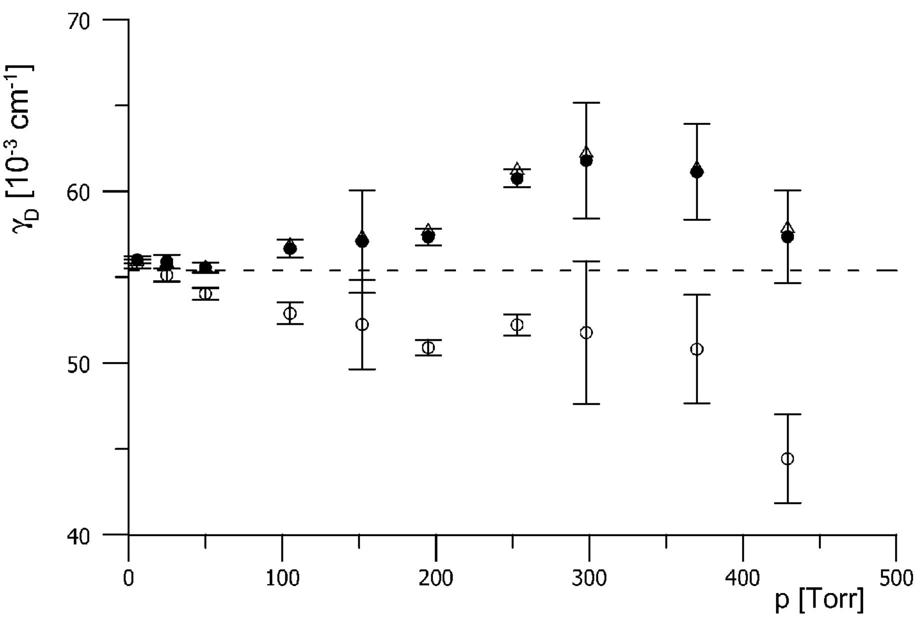

Fig. 2. Plots of the Doppler width γ_D of the 326.1 nm Cd line perturbed by krypton determined from the best fit of the AVP (open circles) and SDAVP (for van der Waals (triangles) and Czuchaj and Stoll (full circles) potentials) to the experimental data, against the pressure of Kr. Dashed line — theoretical Doppler width corresponding to the cell temperature (724 K). Error bars indicate the value of the standard deviation.

In Fig. 2 the Doppler widths γ_D of the 326.1 nm ^{114}Cd line perturbed by Kr are plotted against the Kr pressure. The γ_D values were obtained from numerical fits of AVP (open circles) and SDAVP (triangles and full circles) formulas to the experimental profile. As can be seen, the Doppler width determined by fitting data to AVP using a least-squares minimisation method decreases markedly with increasing Kr pressure. Similar reduction of the Doppler width with increasing pressure of perturbing gas was first experimentally observed by McCartan and Lwin [20] for Li resonance line broadened by Xe and by Harris et al. for the Ca resonance line broadened by Kr [9, 11]. Such a behaviour can be regarded as an evidence of the occurrence of speed-dependent Doppler-collision correlation effects in agreement with theoretical predictions due to Berman [7] and Ward et al. [8]. As already noted, these speed-dependent effects are taken into account in the SDAVP formula which includes the finite duration of collision effect as well.

It must be emphasized that the evaluation of the line shape in terms of SDAVP requires the knowledge of the differences $\Delta V(R)$ of the interaction potentials in the upper $V_u(R)$ and lower $V_l(R)$ states of the emitter. The Cd–Kr system in its ground state ($\mathrm{Cd}(5^1S_0) + \mathrm{Kr}(^1S_0)$) is described by one potential curve X^10^+ only whereas in the excited state ($\mathrm{Cd}(5^3P_1) + \mathrm{Kr}(^1S_0)$) there are two potential curves A^30^+ and B^31. The observed 326.1 nm Cd line is thus a superposition of contributions coming from the $A^30^+ - X^10^+$ and $B^31 - X^10^+$ transitions. The only theoretical potentials for the X^10^+, A^30^+, and B^31 molecular states of the Cd–Kr system are those calculated by Czuchaj and Stoll [13]. In order to perform a SDAVP analysis of our experimental profiles for the 326.1 nm Cd line broadened by Kr we have used both the Czuchaj–Stoll potentials as well as purely attractive van der Waals potential $V(R) = -C_6R^{-6}$. We have also used the Morse potential determined by Koperski et al. [14] from their data on excitation and fluorescence spectra of the CdKr molecule recorded in an experiment of supersonic molecular beam crossed with pulsed dye laser beam. Figure 3 shows the appropriate differences: $\Delta V(R) = V_A - V_X$ and $\Delta V(R) = V_B - V_X$ of molecular potentials describing the A^30^+, B^31 and X^10^+ states, plotted for Czuchaj–Stoll [13], Morse [14], and van der Waals [21] potentials.

In Fig. 2 the values of γ_D marked as triangles were obtained from the analysis in terms of SDAVP assuming the interaction potential in the van der Waals form $V(R) = -C_6R^{-6}$. It should be noted that in the case of inverse-power potentials $V(R) = -C_kR^{-k}$ the reduced B-functions in Eq. (1) are independent of value of the C_k force constant [8, 18, 19].

On the other hand, the values of γ_D marked by full circles in Fig. 2 were determined by the SDAVP analysis assuming $V(R)$ in the form of theoretical potentials calculated numerically by Czuchaj and Stoll [13]. As can be seen from Fig. 2, use of the SDAVP to analyse the data gives acceptable values of the Doppler width at all pressures. The mean value of the Doppler width for pressures below 150 Torr is very close to the theoretical value 55.4×10^{-3} cm^{-1} corresponding to the cell temperature ($T = 724$ K). However, we should note that for Kr pressures between 150 and 450 Torr the values of γ_D obtained by the SDAVP analysis both for the van der Waals and Czuchaj–Stoll potentials are higher than the Doppler width determined from the cell temperature. Moreover, they depend on the pressure.

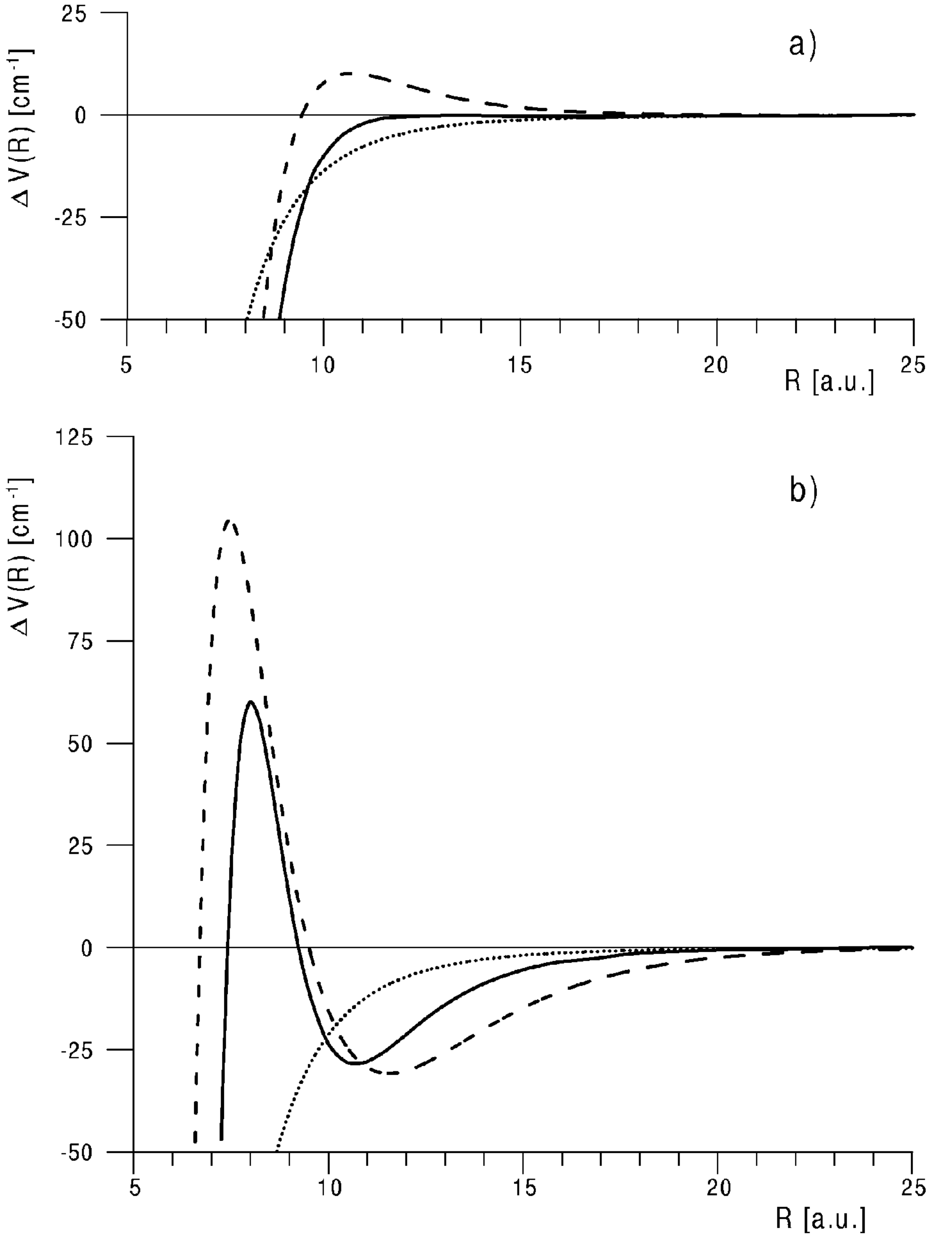

Fig. 3. The differences: (a) $\Delta V(R) = V_A - V_X$ and (b) $\Delta V(R) = V_B - V_X$ of the molecular potentials describing the $A^3 0^+$, $B^3 1$, and $X^1 0^+$ states, plotted for Czuchaj–Stoll (solid line), Morse (dashed line), and van der Waals (dot line) potentials.

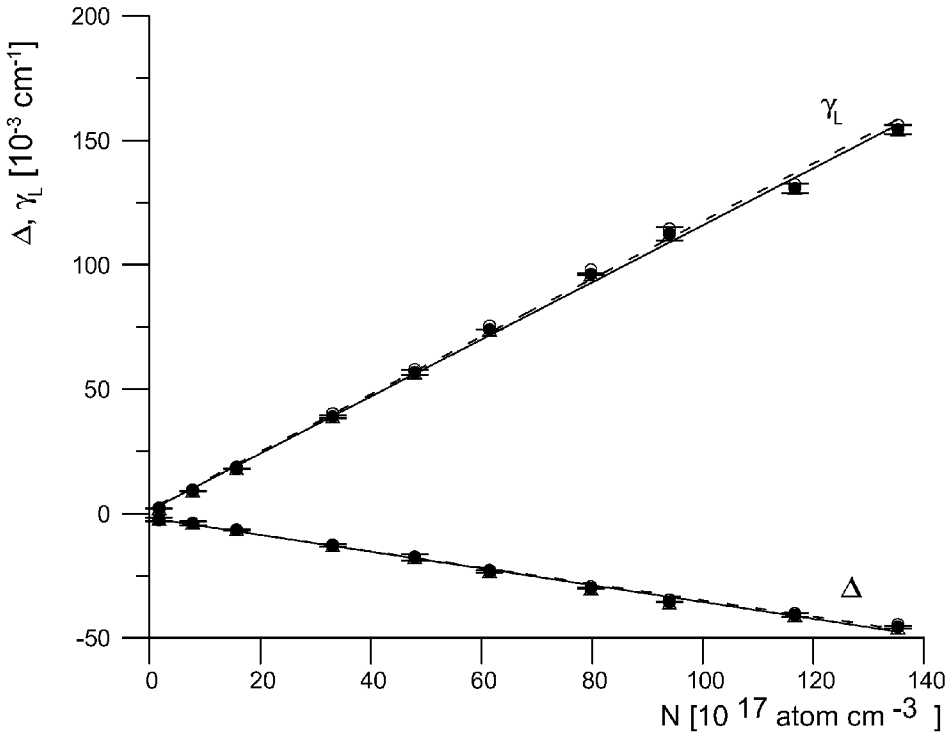

Fig. 4. Plots of the Lorentzian width $\gamma_{\rm L}$ and shift Δ of the 326.1 nm Cd line determined from the best fit of the AVP (open circles and dashed line) and SDAVP (for van der Waals (triangles and dash-and-dot line) and Czuchaj and Stoll (full cirles and solid line) potentials) to the experimental data against the krypton density N. Error bars indicate the value of the standard deviation. For the clarity of the figure we plotted the error bars only for the SDAVP (with Czuchaj and Stoll potential). For two other fits the error values were of the same magnitude.

Figure 4 shows the plots of the Lorentzian width $\gamma_{\rm L}$ and shift Δ determined from the best fit of AVP and SDAVP (with van der Waals and Czuchaj–Stoll [13] potentials) to our experimental profiles against the density number N of krypton. As can be seen, the shift is towards the red and both $\gamma_{\rm L}$ and Δ are linearly dependent on the density. From the slopes of these linear dependencies the pressure broadening $\beta = \gamma_{\rm L}/N$ and shift $\delta = \Delta/N$ coefficients were determined and listed in Table. They are marked "This work AVP", "This work SDAVP-vdW" and "This work SDAVP-CS", respectively.

The experimental values of β and δ determined from these three fitting procedures are different, although they are close to each other. The broadening coefficients obtained by the speed-dependent analysis are only slightly lower (about 1%) than that resulting from the asymmetric Voigt profile analysis. Unlike the broadening, the pressure shift coefficients obtained by the speed-dependent analysis are slightly higher (about 3%) than that obtained for asymmetric Voigt profile.

TABLE

Comparison of experimental values of the β, δ (in units 10^{-20} cm^{-1}/(atom cm^{-3})) and κ (in units 10^{-21}/(atom cm^{-3})) coefficients with those calculated for different interatomic potentials. For experimental data the values of standard deviations are given.

Experimental values	$\beta_{\rm exp}$	$\delta_{\rm exp}$	$\kappa_{\rm exp}$
F-P [12]	1.00(3)	–0.27(3)	–
Abs. [1]	–	–	–0.75(7)
This work AVP	1.159(11)	–0.329(5)	–1.16(7)
This work SDAVP-vdW	1.146(10)	–0.341(5)	–0.94(7)
This work SDAVP-CS	1.147(11)	–0.338(5)	–1.00(7)
Theoretical values	$\beta_{\rm theor}$	$\delta_{\rm theor}$	$\kappa_{\rm theor}$
Czuchaj–Stoll [13]	1.182	–0.181	–0.99
van der Waals	1.064	–0.386	–0.92
Morse	1.838	–0.214	–1.39

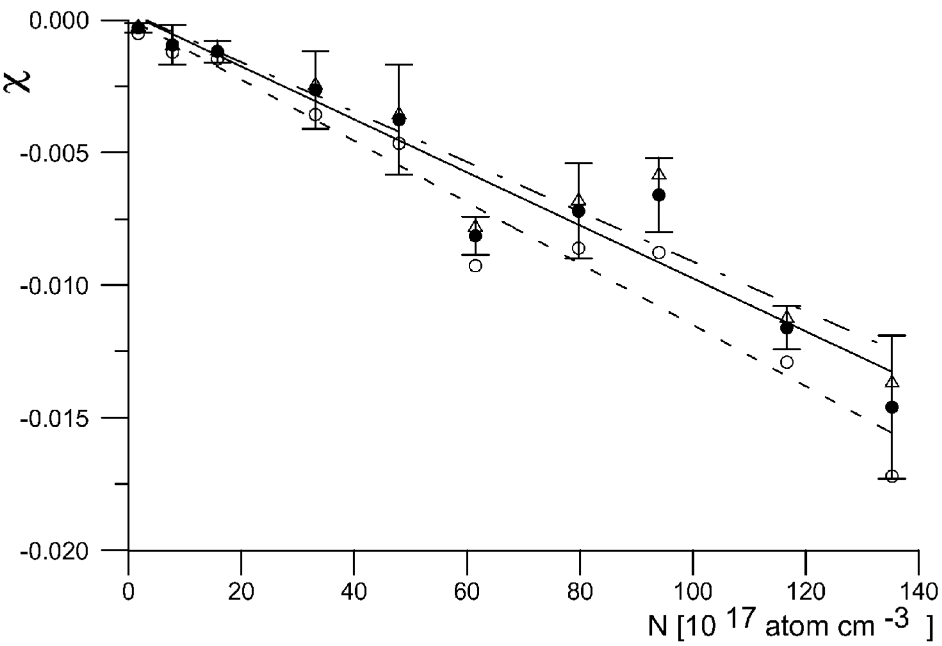

Fig. 5. Plots of the asymmetry parameter χ determined from the best fit of AVP and SDAVP to the experimental data against the krypton density N (notations as in Fig. 3).

Figure 5 shows the plot of the collision-time asymmetry parameter χ which is a measure of the dispersion-shaped contribution to the Lorentzian component of the profile. The values of χ marked by open circles were obtained by fitting the data to AVP formula. The triangles and full circles are the values of χ determined by the SDAVP analysis using either the van der Waals or Czuchaj–Stoll potentials, respectively. As can be seen, the collision-time asymmetry parameter is linearly dependent on the density. From the slope of the best fit straight line the collision-time asymmetry coefficients $\kappa = \chi/N$ were determined and listed in Table. As can be seen from Table, the experimental values of κ coefficients obtained by speed-dependent analysis for van der Waals and Czuchaj–Stoll potentials are close to each other, but they are lower about 15% than that resulting from the asymmetric Voigt profile analysis in which speed-dependent effects were neglected.

4. Discussion

In the present work we have shown that though the SDAVP can be fitted well to our experimental profiles (see Fig. 1), the values of the best-fit Doppler width γ_D obtained by the SDAVP analysis above 150 Torr for van der Waals and Czuchaj–Stoll potentials are dependent on Kr pressure. The reason of such a dependence is not clear. We should emphasize, however, that SDAVP still represents an approximate expression only. First of all, it should not be forgotten that the SDAVP formula was derived assuming that the velocity-changing collisions which, in principle, can lead to the Dicke narrowing [22] of the Doppler component of the line profile can be neglected. On the other hand, however, the values of best-fit Doppler width γ_D obtained by the SDAVP analysis are higher than the value corresponding to the cell temperature and no additional decrease in the Doppler width which could be caused by the Dicke narrowing was observed in our experiment. It means that in this case the inclusion of velocity-changing collisions would not improve the results. We can thus conclude that this disagreement may be caused by the fact that neither van der Waals nor Czuchaj–Stoll potentials give correct description of the Cd–Kr interaction. We should note that for some other atomic systems such as Ca perturbed by rare gases [9, 11, 23], Ne [24] and Ar [25] perturbed by Ne, and Cd perturbed by Xe [10, 26] the observed line shapes were also successfully interpreted in terms of SDAVP or SDVP expressions in which the Dicke narrowing was omitted. Therefore also in the present work the final analysis of our experimental data was performed using the SDAVP formula.

The experimental values of pressure broadening β, shift δ, and asymmetry κ coefficients determined in the course of the present work are listed in Table. In a previous work [12] from this laboratory the β and δ coefficients for the 326.1 nm Cd line perturbed by Kr were determined using a classical emission spectroscopy technique, i.e. by means of a pressure scanned FPI for the cell temperature $T =$ 468 K. The values of β and δ obtained in this way are listed in Table where they are marked as "F-P [12]". As can be seen from Table, there is a small temperature dependence consisting in the increase in β and δ coefficients with the increase in cell temperature from $T = 468$ K to $T = 724$ K, which is in agreement with theoretical predictions. This is, however, in contrast with the results obtained for Cd–Xe [10] and Cd–Ar [27] systems where no temperature dependence was found.

In order to interpret our experimental data we calculated the theoretical values of pressure broadening β and shift δ coefficients on the basis of the adiabatic phase-shift theory with straight-line trajectories [5] using equation (3) in II for different interaction potentials. We performed calculations for the Czuchaj and Stoll [13] numerical potential as well as for two potentials derived from experimental data i.e. for van der Waals potential with the same constants (determined by Grycuk et al. [21]) as used in Ref. [12] and for Morse potential with the spectroscopic constants determined recently by Koperski et al. [14].

The values of β and δ coefficients evaluated for these potentials are listed in Table and marked as "Czuchaj–Stoll [13]", "van der Waals" and "Morse", respectively. As can be seen from Table, our experimental value of β is in reasonable agreement with theoretical one calculated on the basis of the Czuchaj–Stoll [13] potential. For the line shift there is rather poor agreement for the value calculated for van der Waals potential while the values obtained for the Morse and Czuchaj–Stoll potential are much lower than the experimental ones.

The experimental values of collision-time asymmetry coefficients κ determined in the course of the present work are listed in Table, where they are compared with theoretical values. In paper I the collision-time asymmetry coefficient κ for the 326.1 nm Cd line perturbed by Kr was determined using a classical absorption spectroscopy technique and this value is listed in Table and marked "Abs. [1]". As can be seen from Table, this κ value is about 25% lower than the value obtained in the present work. The reasons of this disagreement seem to be twofold. Firstly, there is too low resolution of the used monochromator and secondly, the systematic error due to its instrumental function. The monochromator used in measurements reported in I was built in the so-called vertical Ebert mounting (for details see [28] and references therein). This type of spectrograph is affected by spectral line tilt and spectral line curvature effects which lead to the asymmetry of its instrumental function. Since the instrumental function cannot be described by analytical formula, it was determined in experimental way [1]. It should be noted, however, that such a rather rough approximation to the real instrumental function may breed errors in the line shape analysis, especially for the line asymmetry, since this effect is rather small.

In paper II we have also shown that in the case of the van der Waals potential the values of the asymmetry parameter calculated in the framework of the unified Franck–Condon treatment [3, 6] are very close to that resulting from the Anderson–Talman approach [2, 29]. It should be noted, however, that Eq. (10) in paper II is more convenient for numerical application, especially in averaging over Maxwellian distribution of velocities, than other known expressions [3, 30]. As can be seen from Table, good agreement between our experimental and theoretical values of the asymmetry coefficient κ takes place for the Czuchaj–Stoll [13] as well as for the van der Waals potential. The poor agreement is obtained, however, for the Morse potential.

5. Conclusion

In this work we have shown that for the Cd–Kr system with the perturber-emitter mass ratio $\alpha = 0.73$ the neglect of the speed-dependence of the collisional width and shift may cause errors in the values of the Doppler width and collision-time asymmetry parameter determined from the line shape analysis. It should be noted that it is not often to observe the correlation between the collision and Doppler broadening for the systems with the perturber-emitter mass ratio $\alpha \leq 1$. However, in previous experiments we observed such a correlation for the Ar–Ne system $\alpha = 0.5$ [25].

The inclusion of the speed-dependent effects with the assumption of the Czuchaj–Stoll [13] or the van der Waals potential increases the underestimated values of best-fit Doppler widths, but does not cancel the dependence of the Doppler width on the perturber pressure. It implies that neither van der Waals nor Czuchaj–Stoll potentials give correct description of the Cd–Kr interaction.

The comparison of pressure broadening, and asymmetry coefficients determined in this experiment with coefficients calculated on the basis of the adiabatic semiclassical approach shows a good agreement between experimental and theoretical values obtained for numerical potentials calculated by Czuchaj and Stoll [13]. The value of the pressure shift coefficient obtained for the Czuchaj and Stoll potential is almost twice lower than the experimental value. Taking into account that the value of the pressure shift coefficient obtained for the van der Waals potential is much closer to the experimental value, we can thus conclude that Czuchaj and Stoll [13] potential is not appropriate at the larger interatomic distances which mainly influence on the line shift. A poor agreement between experimental and theoretical values was obtained for the Morse potential.

Acknowledgment

The authors wish to express their gratitude to Professor J. Szudy for valuable help in the preparation of the manuscript.

References

[1] J. Domysławska, A. Bielski, R.S. Trawiński, *J. Quant. Spectrosc. Radiat. Transf.* **61,** 735 (1999).

[2] P.W. Anderson, J.D. Talman, in: *Conference on Broadening of Spectral Lines*, University of Pittsburg, unpublished (1955); *Bell Teleph. Syst. Tech. Publ.* No. 3117.

[3] J. Szudy, W.E. Baylis, *J. Quant. Spectrosc. Radiat. Transf.* **15,** 641 (1975); **17,** 681 (1977).

[4] B.N.I. Al-Saqabi, G. Peach, *J. Phys. B* **20,** 1175 (1987).

[5] N. Allard, J. Kielkopf, *Rev. Mod. Phys.* **54,** 1103 (1982).

[6] J. Szudy, W.E. Baylis, *Phys. Rep.* **266,** 127 (1996).

[7] P.R. Berman, *J. Quant. Spectrosc. Radiat. Transf.* **12,** 1331 (1972).

[8] J. Ward, J. Cooper, E.W. Smith, *J. Quant. Spectrosc. Radiat. Transf.* **14,** 555 (1974).

[9] M. Harris, E.L. Lewis, D. McHugh, I. Shannon, *J. Phys. B* **17,** L661 (1984).

[10] A. Bielski, R. Ciuryło, J. Domysławska, D. Lisak, R.S. Trawiński, J. Szudy, *Phys. Rev. A* **62,** 032511 (2000).

[11] I. Shannon, M. Harris, D. McHugh, E.L. Lewis, *J. Phys. B* **19,** 1409 (1986).

[12] S. Brym, J. Domysławska, *Phys. Scr.* **52,** 511 (1995).

[13] E. Czuchaj, H. Stoll, *Chem. Phys.* **248,** 1 (1999).

[14] J. Koperski, M. Łukomski, M. Czajkowski, in: *Spectral Line Shapes*, Vol. 11, Ed. J. Seidel, American Institute of Physics, New York 2001, in print.

[15] A. Bielski, R. Ciuryło, J. Domysławska, D. Lisak, R.S. Trawiński, J. Wolnikowski, *Acta Phys. Pol. A* **97,** 1003 (2000).

[16] R.E. Walkup, A. Spielfiedel, D. Ely, W.D. Phillips, D.E. Pritchard, *J. Phys. B* **14,** 1953 (1981).

[17] M. Harris, E.L. Lewis, D. McHugh, I. Shannon, *J. Phys. B* **19,** 3207 (1986).

[18] R. Ciuryło, J. Szudy, R.S. Trawiński, *J. Quant. Spectrosc. Radiat. Transf.* **57,** 551 (1997).

[19] R. Ciuryło, *Phys. Rev. A* **58,** 1029 (1998).

[20] D.G. McCartan, N. Lwin, *J. Phys. B* **10,** L17 (1977).

[21] T. Grycuk, M. Findeisen, A. Śniecińska, in: *Spectral Line Shapes*, Vol. 6, Eds. L. Frommhold, J.W. Keto, American Institute of Physics, New York 1990, p. 174.

[22] R.H. Dicke, *Phys. Rev.* **89,** 472 (1953).

[23] E.L. Lewis, in: *Spectral Line Shapes*, Vol. 5, Ed. J. Szudy, Ossolineum Publishing, Wrocław 1988, p. 485.

[24] R. Ciuryło, A. Bielski, S. Brym, J. Domysławska, D. Lisak, J. Szudy, R.S. Trawiński, *Acta Phys. Pol. A* **96,** 359 (1999).

[25] A. Bielski, S. Brym, R. Ciuryło, J. Szudy, *Eur. Phys. J. D* **8,** 177 (2000).

[26] S. Brym, R. Ciuryło, R.S. Trawiński, A. Bielski, *Phys. Rev. A* **56,** 4501 (1997).

[27] A. Bielski, D. Lisak, R.S. Trawiński, *Eur. Phys. J. D*, in print.

[28] R.S. Trawiński, J. Domysławska, R. Ciuryło, A. Bielski, *Appl. Opt.* **32,** 4828 (1993).

[29] G. Traving, *Über die Theorie der Druckverbreiterung von Spektrallinien*, Verlag G. Braun, Kalsruhe 1960.

[30] A. Royer, *Acta Phys. Pol. A* **54,** 805 (1978).